

Diversity and Decoding in Non-Ideal Conditions

(Chun-Ye) Susan Vasana, Ph.D.
University of North Florida
United States

1. Introduction

Nowadays, there are many products that provide personal wireless services to users who are on the move. Multiple antenna diversity is usually required to make a wireless link more reliable. User terminals have to be small enough to consume and emit low power. As a result, antennas cannot be spaced far apart enough to have independent and diverse branches for the received signals. Another issue affecting diversity gain is the unbalanced branches due to different locations or different polarizations of the antennas. The average signal power received from those unbalanced branches is different. Both the branch correlation and power imbalance degrade the benefits of diversity reception. Therefore, it is very important to investigate such effects before applying diversity reception to practical mobile or wireless radio systems.

There have been a significant numbers of theoretical researches reported in the area of diversity systems and combining techniques. Some papers considered diversity systems with the correlated branches as in the references. The problems of correlated and unbalanced branches are addressed in (Dietze et al., 2002) and (Mallik et al., 2002) for the two-branch diversity system and for the Rayleigh fading channel. This chapter will address both the effects of branch correlation and power imbalance for generic L branches diversity system. The diagonalization transformation is used in the performance analysis for diversity reception with the correlated Rayleigh-fading signals in (Fang et al., 2000)-(Chang & McLane, 1997). Here, the diagonalization transformer is introduced as a linear transformer implemented before the diversity branches are being combined, which can transform the correlated and balanced branches to the uncorrelated and unbalanced ones, and vice versa. A real world simulation system is included in the chapter, which has the extended result of the paper (Vasana & McLane, 2004).

Most analyses assume that the fading signal components are correlated in diversity branches but the noise components are independent in the branches. However, the external noise and interference that come with the fading signals are correlated. Plus, the coupling of diversity branches has the same effect on both signal and noise components. Some paper assumes that the dominant noise and interference have the same correlation distribution as the fading signals (Chang & McLane, 1997). This chapter assumes a generic case, in which the noise components are correlated with a correlation equal or smaller than the correlation between signal components. If the transmitted signal is $u(t)$, the received signal from the k^{th} branch can be expressed as:

$$r_k(t) = A_k u(t) + n_k(t) = s_k(t) + n_k(t) \quad k=1, 2, \dots, L \quad (1)$$

where:

$$A_k = R_k e^{-j\Phi_k}, \quad k=1, 2, \dots, L \quad (2)$$

is the complex, fading phasor of $r_k(t)$. And $n_k(t)$ is the additive white Gaussian noise and interference component. For the Rayleigh or Rician fading channels, the envelope of the received signal, R_k , in the first term of equation (1) can be approximately described by the Rayleigh or Rician distribution, depending on if there is or not a major stable line-of-sight (LOS) path between the transmitter and the receiver. In both cases, the complex fading phasor, A_k , $k=1, 2, \dots, L$, are complex correlated Gaussian random variables. So is the first term, $A_k u(t)$, in equation (1) as $u(t)$ is a deterministic transmitted signal.

With the fading model in equations (1) and (2), the fading signal components received in k^{th} antennas, $s_k(t)$, $k=1, 2, \dots, L$, are complex Gaussian processes with real and imaginary components, X_k and Y_k , both with zero mean for the Rayleigh fading, and non-zero mean for the Rician fading. For the simplicity of analysis, assume that the L branches have identical correlation coefficient and there is no cross correlation between any in-phase and quadrature-phase components. There are only correlation coefficients between any two diversity branches, ρ , which is related to the antenna distance and coupling effects.

2. The conversion between correlation and imbalance among diversity branches

The same effect to the diversity gain was measured with either correlation between diversity branches or power imbalance among the branches. A linear transformation can transform one situation to another.

2.1 Diagonalization transformation

The diagonalization technique has been used successfully in the error performance analysis for diversity with correlated branches (Fang, etc. 2000) and (Chang & McLane, 1997). Here the diagonalization technique is used as a transformer at the diversity reception. The intent is to develop a simple linear system to deal with the correlated or unbalanced branches in diversity systems, and maximize diversity gain by combining methods under different situations (Vasana, 2008).

Assuming the correlation coefficients among the L branches is identical, and the average power of the received signal components for each branch is identical to $2\sigma_s^2$. Furthermore, the correlation distribution between in-phase components is the same as the correlation between quadrature-phase components. Under the above assumption, the covariance matrix C_X or C_Y for the signal components, X_k and Y_k , is symmetric as:

$$C_X = C_Y = \sigma_s^2 \begin{pmatrix} 1 & \rho_s & \rho_s & \dots & \rho_s \\ \rho_s & 1 & \rho_s & \dots & \rho_s \\ & & \dots & & \\ \rho_s & \rho_s & \rho_s & \dots & 1 \end{pmatrix} \quad (3)$$

The linear transformation between the received signal vector $R = [r_1, r_2, \dots, r_L]$ and transformed signal vector $Z = [z_1, z_2, \dots, z_L]$ is:

$$\left\{ \begin{array}{l} z_1 = \xi_1^{(1)}r_1 + \xi_2^{(1)}r_2 + \dots + \xi_L^{(1)}r_L \\ z_2 = \xi_1^{(2)}r_1 + \xi_2^{(2)}r_2 + \dots + \xi_L^{(2)}r_L \\ \dots \\ \dots \\ z_{L-1} = \xi_1^{(L-1)}r_1 + \xi_2^{(L-1)}r_2 + \dots + \xi_L^{(L-1)}r_L \\ z_L = (r_1 + r_2 + \dots + r_L) / \sqrt{L} \end{array} \right. \quad (4)$$

where $[\xi_1^{(i)}, \xi_2^{(i)}, \dots, \xi_L^{(i)}]$ for $i=1, 2, \dots, L-1$ are eigenvectors of the covariance matrix in equation (3). As an example of $L=3$ diversity systems, the transformation in equation (4) was given in (Vasana, 2008).

After the transformation as in equation (4), the the covariance matrix C_{Z_r} or C_{Z_i} for the real and imaginary signal components, Z_r and Z_i , of the trnasformed signal vector Z , is diagonalized as follow:

$$C_{Z_r} = C_{Z_i} = \sigma_s^2 \begin{pmatrix} 1-\rho_s & 0 & 0 & \dots & 0 & 0 \\ 0 & 1-\rho_s & 0 & \dots & 0 & 0 \\ & & \dots & & & \\ 0 & 0 & 0 & \dots & 1-\rho_s & 0 \\ 0 & 0 & 0 & 0 & \dots & 1+(L-1)\rho_s \end{pmatrix} \quad (5)$$

The diagonalized covariance matrix above indicates there are no corrleation between L transformed branches. The values in the diagnoal of the matrix (5) are the eigenvalues of the covariance matrix (3) of the signal vector before the transformation, which indicates the average signal power in each branches. Equation (5) shows that after the transformation the first $(L-1)$ branches have the same average power but the L th branch has the different average power from the others. The diagonalization transformation can be expressed in the following blockdiagram. The diagonalizer transformer in the Fig. 1 is a linear transformation between vector R and Z by equation (4), using the eigenvector derived from the convariance matrix in (3).

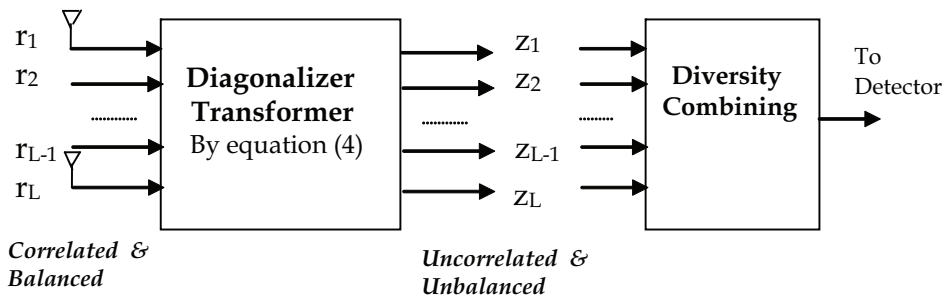


Fig. 1. Diagonalizer (Transformer) Block Diagram

The outputs of the transformer are a set of uncorrelated complex Gaussian random processes with λ_i as their variance values. That is, using the diagonalizer, the L branch correlated random processes have been transformed to the L branch uncorrelated random processes. However, the average signal power of each branch will not be the same, but are the twice of the values in the diagonal position of the matrix in (5) as follow:

$$\begin{cases} (P_s)_i = (P_x)_i + (P_y)_i = 2\sigma_s^2(1 - \rho_s), & i = 1, 2, \dots, L-1 \\ (P_s)_L = (P_x)_L + (P_y)_L = 2\sigma_s^2[1 + (L-1)\rho_s] \end{cases} \quad (6)$$

The noise and interference components, $n_k(t)$, $k=1, 2, \dots, L$, of the received signal $r_k(t)$, $k=1, 2, \dots, L$, in equation (1) have the same correlation distribution as in equation (3) but with smaller correlation coefficient ρ_n and average noise power σ_n^2 . At the outputs of the transformer, the noise components will be similarly de-correlated. Hence, the average signal-to-noise ratios (SNR) in the L branches at the output of the transformer will be:

$$\begin{cases} (P_s / P_n)_i = \frac{\sigma_s^2(1 - \rho_s)}{\sigma_n^2(1 - \rho_n)} & i = 1, 2, \dots, L-1 \\ (P_s / P_n)_L = \frac{\sigma_s^2[1 + (L-1)\rho_s]}{\sigma_n^2[1 + (L-1)\rho_n]} \end{cases} \quad (7)$$

From the above equations, the followings can be concluded:

1. Before the transformation the signal-to-noise ratios (P_s / P_n) are the same for all L branches, which is σ_s^2 / σ_n^2 for the power balanced L branches.
2. After the transformation the signal-to-noise ratio (P_s / P_n) of the Lth branch is enhanced usually as $\rho_s > \rho_n$. The Lth branch is the combinational branch just as what the equal-gain combining method does.
3. After the transformation the signal-to-noise ratios $(P_s / P_n)_i$ of the 1st to (L-1)th branches are reduced as $\rho_s > \rho_n$. They can provide (L-1) balanced diversity branches as the SNR are the same in all the (L-1) branches.

2.2 Discussion of different diversity conditions

This section illustrates the magic transformation between correlation and power imbalance of diversity branches. The diagonalizer is derived and is introduced here before the diversity branches are combined, which can transform the correlated and balanced branches to the uncorrelated and unbalanced ones, and vice versa. This section assumes a generic model, in which noise and interference components are correlated with a correlation equal to or less than the correlation of signal components. Modeling and simulation of an example and the performance can be found for various dual diversity scenarios in (Vasana, 2008). Discussions on how to maximize diversity gains are made in various signal and noise conditions, and with different combining methods as following cases.

Case 1: $\rho_s = \rho_n$

Resulted from the system analysis and simulation, this technology is especially effective when the noise/interference components have the same correlation as the signal components, i.e. $\rho_s = \rho_n$. This is the case when interferences, which come along with the

desired signal, are the main source of noise, such as the cases in CDMA (Code Division Multiple Access) systems and wireless networks, etc. In such as the diagonalizer described in this section can be viewed as a “decorrelator” - to totally straighten the correlation effect and resulted balanced signal-to-noise ratio among diversity branches in those practical non-ideal scenarios. The equation (7) with $\rho_s = \rho_n$ becomes

$$\begin{cases} (P_s / P_n)_i = \sigma_s^2 / \sigma_n^2, & i = 1, 2, \dots, L-1 \\ (P_s / P_n)_L = \sigma_s^2 / \sigma_n^2 \end{cases} \tag{8}$$

The outputs at the transformer will have unequal signal or noise power distribution as in (6) but balanced signal-to-noise ratio among the diversity branches as in (8). It is the ideal situation to use the diagonalizer. The diversity gain will be maximized with the use of the diagonalizer. The average signal-to-noise ratio in each diversity branch at both inputs and outputs of the transformer are the same, $(P_s / P_n)_i = \sigma_s^2 / \sigma_n^2$, for $i = 1, 2, \dots, L$.

Case 2: $\rho_s \gg \rho_n$

If the correlation between signal components is much greater than the correlation between noise components among the diversity branches, i.e. $\rho_s \gg \rho_n$, the average signal-to-noise ratio (P_s / P_n) at the output of the transformer will be enhanced in the L^{th} branch z_L . This last branch at the output of the transformer, z_L , alone can be used as the combined diversity branch. It can be seen in (9) by substituting $\rho_s \gg \rho_n$ in the equation (7):

$$\begin{cases} (P_s / P_n)_i \approx \frac{\sigma_s^2(1 - \rho_s)}{\sigma_n^2} & i = 1, 2, \dots, L-1 \\ (P_s / P_n)_L \approx \frac{\sigma_s^2[1 + (L-1)\rho_s]}{\sigma_n^2} \end{cases} \tag{9}$$

Case 3: $\rho_n = 0$

There is extreme case when the noise components are uncorrelated and balanced among the branches. Substituting $\rho_n = 0$ to equation (7) it becomes:

$$\begin{cases} (P_s / P_n)_i = \frac{\sigma_s^2(1 - \rho_s)}{\sigma_n^2} & i = 1, 2, \dots, L-1 \\ (P_s / P_n)_L = \frac{\sigma_s^2[1 + (L-1)\rho_s]}{\sigma_n^2} \end{cases} \tag{10}$$

In such case, the diagonalization transformation has no effect on the noise components. The signal components will become unbalanced after the transformation, but the noise components are still independent and balanced. If the correlation is evenly distributed among the L diversity branches, the $(L-1)$ branches will still be balanced after the transformation as in (6). Diversity gain can be achieved by using these $(L-1)$ uncorrelated and balanced branches at the output of the diagonalizer transformer, practically when L is at least greater than 3. However, it can be seen from equation (10) that the reduced signal-to-noise ratio needs to be considered in these $(L-1)$ transformed branches, while the last L^{th} transformed branch has an increased signal-to-noise ratio.

Case 4: $\rho_s = \rho_n = 0$, but unbalanced branches ($\sigma_{r1}^2 = q \sigma_{r2}^2$)

The transformation in equation (4) is a two-way transformation. It is meant that it can transform not only a set of correlated & balanced branches to a set of uncorrelated & unbalanced ones, but also a set of unequal power branches (unbalanced) & uncorrelated branches to a set of balanced & correlated branches. With the revised condition of uncorrelated but unbalanced diversity branches to be transformed, the block diagram in Fig.1 becomes Fig. 2.

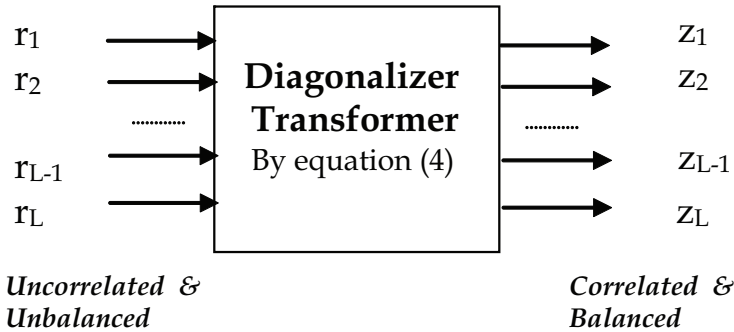


Fig. 2. Diagonalizer (Transformer) Block Diagram (w/. revised condition)

To illustrate this point by using an example of dual diversity ($L=2$), let r_1 and r_2 be the uncorrelated but unbalanced diversity branches, and the average power of r_1 is q times that of r_2 , where $0 < q < 1$. After the transformation for dual diversity ($L=2$) z_1 and z_2 in equation (4) is as simple as:

$$\begin{cases} z_1 = (r_1 + r_2) / \sqrt{2} \\ z_2 = (r_1 - r_2) / \sqrt{2} \end{cases} \tag{11}$$

z_1 and z_2 are correlated but with equally average power as:

$$\begin{cases} \sigma_{z1}^2 = (\sigma_{r1}^2 + \sigma_{r2}^2) / 2 \\ \sigma_{z2}^2 = (\sigma_{r1}^2 + \sigma_{r2}^2) / 2 \end{cases} \tag{12}$$

and the correlation coefficient as:

$$\rho_{z1z2}(\%) = \frac{E(z_1 z_2)}{\sigma_{z1} \sigma_{z2}} = \frac{\sigma_{r1}^2 - \sigma_{r2}^2}{\sigma_{r1}^2 + \sigma_{r2}^2} = \frac{1 - q}{1 + q} \tag{13}$$

where the power imbalance ratio q between r_1 and r_2 can be expressed in decible:

$$q(\text{dB}) = 10 \log (q) \tag{14}$$

Thus, the diversity system with unequal average signal power can be transformed to the correlated diversity system with balanced diversity branches.

For maximal-ratio combining, the performance of the diversity system with or without the diagonalizer is the same, as in (Fang et al., 2000), (Loyka et al., 2003) and (Bi et al., 2003). The L^{th} branch at the output of the transformer gives an equal-gain combining of the original correlated branches. For square-law combining, the performance analysis using diagonalization technique is illustrated in detail in (Chang & McLane, 1997).

2.3 The simulation results

A switch algorithm, which is discussed in Section 4, is simulated to combine two diversity branches in various cases. The Rayleigh fading channel is considered in the simulation. The envelopes of faded signals in two diversity branches are shown as the first two signals in the Fig 3 (Vasana, 2008). This is the case when there is 90% correlation between two diversity branches. The combined signal envelop is shown in the 3rd signal in the Fig 3, in which many deep fading dips are avoided.

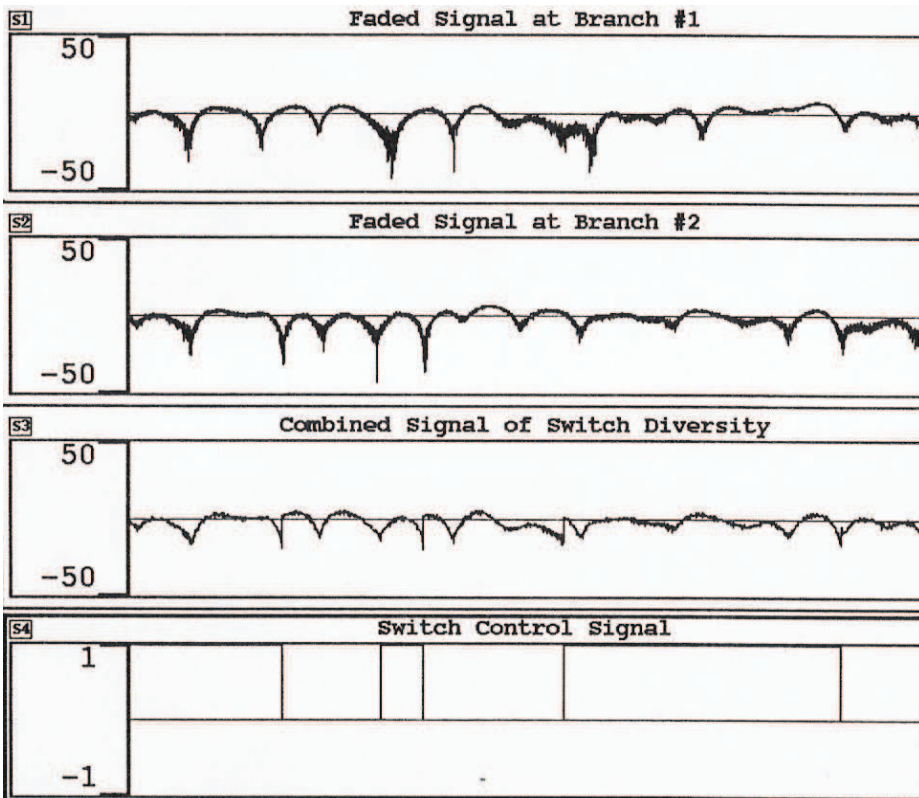


Fig. 3. Fading Signal Envelopes in Diversity Branches ($L=2$)

From the other simulation results of symbol-error-rate (SER) or the average bit-error-rate (BER) listed in the Table of (Vasana, 2008), the following comparison and conclusions can be obtained:

1. Dual antenna diversity is better than no diversity, even with high correlation ($\rho_s = 90\%$) or high power imbalance (5dB) between the diversity branches.
2. Correlation or imbalance issues between branches degrade the diversity gain in a similar manner, e.g. 50% correlation case has the same performance as 3dB imbalance case.

In summary, a linear transformer, which diagonalizes the covariance matrix of the diversity branches, is presented and investigated in this section. Not only this diagonalizer can transfer the correlated and balanced diversity branches to the uncorrelated and unbalanced branches, but also can transfer the unbalanced and uncorrelated diversity branches to the balanced and correlated branches. The combining method can be chosen, depending on which situation gives the best performance. Simulation results and the intuitive explanation of switch diversity with dual antenna branches are shown here. This transformation technology is especially effective when the noise components have the same correlation as the signal components. This is the cases when interferences which come along with the desired signal are the main source of noise, such as the cases in CDMA systems and wireless networks, etc. The method described in this section can act like a "filter" - to totally filter out the correlation among diversity branches in these cases.

3. The soft-decision decoding in correlated diversity combining

This section adds another mechanism in combating wireless channel fading - combining convolutional coding with antenna diversity. The method and its performance of the combination of convolutional decoding and antenna diversity with square-law combining on a Rayleigh fading channel are presented here. The diversity branches are correlated or power imbalanced; and the Viterbi soft-decision decoding is performed at the receiver detection. The upper bound performance of the non-coherent detection systems has been determined with the above conditions. Our analysis holds for any number of diversity branches but the computations presented here are for dual diversity. The performance shows the combining of error-correction coding and diversity is very effective even in non-ideal diversity conditions.

3.1 The soft-decision detection

The encoder accepts k binary digits at a time and puts out n binary digits in the same time interval. Thus the code rate is $R_c = k/n$. When the Viterbi decoding algorithm is used, the optimum decoding algorithm for a convolutional encoded sequence transmitted over a memoryless channel is used in the paper (Viterbi & Omura, 1979).

In the system block diagram of Fig. 4, the diversity transformer is the diagonalization transformation discussed in Section 2 to transform correlated & balanced diversity branches to uncorrelated & unbalanced diversity branches. In addition, soft-decision decoding with non-coherent detection is used in this section, which uses square-law combining to provide the decoding variables from the transformed uncorrelated signals received original from L correlated antennas. The notations here can also be found in (Modestino & Mui, 1976, Gradshcheyn & Ryzhik, 1980) .

From (Chang & McLane, 1997) the normalized fading signals at the receiver front-end with matched filters at k th diversity branch are:

$$\begin{cases} r_{0k} = 2\bar{E}_b R_k e^{-j\Phi_k} + N_{0k} \\ r_{1k} = N_{1k} \end{cases} \tag{15}$$

where binary bit 0 is assumed to be transmitted. The r_{0k} are the outputs from the filters matched to the transmitted signal and r_{1k} are the outputs that only include AWGN components.

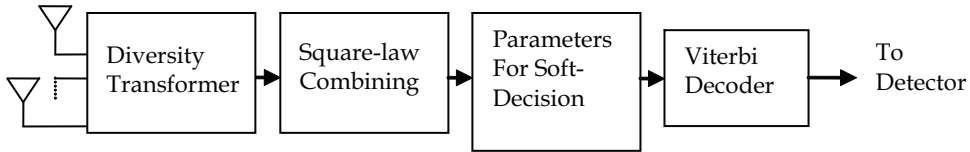


Fig. 4. Soft-Decision Detection Block Diagram

For non-coherent orthogonal demodulation, the output of the square-law combiner with L diversity branches is given by following equation:

$$\begin{cases} y_{0jm} = \sum_{k=1}^L |2\bar{E}_b R_k e^{-j\Phi_k} + N_{0jmk}|^2 = \sum_{k=1}^L |r_{0k}|^2 = \sum_{k=1}^L |z_{0k}|^2 \\ y_{1jm} = \sum_{k=1}^L |N_{1jmk}|^2 = \sum_{k=1}^L |r_{1k}|^2 = \sum_{k=1}^L |z_{1k}|^2 \end{cases} \tag{16}$$

where z_{0k} and z_{1k} are the diagonalized random variables as in (4) that have been transformed from the correlated diversity branches r_{0k} and r_{1k} for $k = 1, 2, \dots, L$ for respective matched filter outputs. It can be proven that the square-law combining gives the same output for combining the branches whether at the input or the output of the diagonalizer transformer using the transformation of (4). In equation (16) the z_{0k} and z_{1k} are uncorrelated Gaussian random variables with zero mean and variances equal to the eigenvalues of the covariance matrix as in (3), and so are the values of the signal power in each branches after the diagonalization transformation as in (6). In equation (6) ρ_s is the correlation between L diversity antennas in the receiver.

The input sequence to the Viterbi decoder, which is the output from the square-law combining, are $\{y_{jmv} \mid m=1, 2, \dots, n; j=1, 2, \dots\}$ for the j -th trellis branch and the m -th bit in that branch. The coded binary digits are denoted by $\{c_{jmv} \mid m=1, 2, \dots, n; j = 1, 2, \dots\}$ for the j -th trellis branch and the m -th bit in that branch. The Viterbi soft-decision decoder (Viterbi & Omura, 1979) with non-coherent detection forms the branch metrics as

$$\mu_j^{(r)} = \sum_{m=1}^n [c_{jm}^{(r)} y_{1jm} + (1 - c_{jm}^{(r)}) y_{0jm}] \tag{17}$$

Furthermore, a metric for the r -th path consisting of B branches through the trellis is defined as:

$$U^{(r)} = \sum_{j=1}^B \mu_j^{(r)} \tag{18}$$

where r denotes any one of the competing paths at each node. For example, the all-zero path, denoted as $r=0$, has a path metric

$$U^{(0)} = \sum_{j=1}^B \sum_{m=1}^n y_{0jm} \quad (19)$$

3.2 The error performance upper bound

Assume that perfect interleaving is used so that there is no fading correlation between consecutive coded symbols. The probability of error in the pairwise comparison of the metrics $U^{(0)}$ and $U^{(r)}$ is

$$P_2(d) = \Pr \left[\sum_{i=1}^d y_{1i} > \sum_{i=1}^d y_{0i} \right] = \Pr [\mu_r \geq \mu_0], \quad (20)$$

where d is the Hamming distance for error events in the code trellis. The bit error probability of binary codes is upper-bounded for $k=1$ (no diversity) as

$$\bar{P}_b < \sum_{d=d_{\text{free}}}^{\infty} \beta_d P_2(d) \quad (21)$$

where β_d is given in (Chang & McLane, 1995).

On making use of (16),

$$\mu_0 = \sum_{i=1}^d y_{0i} = \sum_{i=1}^d \sum_{k=1}^L |2\bar{E}_b R_k e^{-j\Phi_k} + N_{0ik}|^2 \quad (22)$$

and

$$\mu_r = \sum_{i=1}^d y_{1i} = \sum_{i=1}^d \sum_{k=1}^L |N_{1ik}|^2 \quad (23)$$

$$P_2(d) = \int_0^{\infty} f_{\mu_0}(\mu_0) \left[\int_0^{\mu_0} f_{\mu_r}(\mu_r) d\mu_r \right] d\mu_0 \quad (24)$$

For Rayleigh fading, the probability density function of μ_0 and μ_r in equation (24), $f_{\mu_0}(\mu_0)$ and $f_{\mu_r}(\mu_r)$, can be found in (Chang & McLane, 1995).

3.3 The numerical results

Consider a simple convolutional code with constraint length $K_c=3$, code rate $R_c=1/2$, and perfect interleaving is assumed. For a fair comparison with uncoded system, the average signal energy per information bit for the coding system is used, which is denoted as \bar{E}_b . The average SNR corresponding to an information bit, γ_b , is related with the average SNR used through the analysis as (Proakis, 1989) $\gamma_b = \gamma_c / R_c$.

The union bound has been calculated for this $K_c=3$, $R_c=1/2$ convolutional code plus dual diversity with correlation by using the equations (21) - (24) as detailed in (Chang & McLane,

1995). The performance of the $K_c=3$, $R_c=1/2$ convolutional code plus a dual diversity system is compared with the coding system alone.

Numerical calculation of the performance of a $K_c=3$, $R_c=1/2$ convolutional code plus correlated diversity with $L=2, 4$ and 6 and various correlation coefficient as well as the comparison with coding alone system or the diversity alone system are presented in the plots in (Chang & McLane, 1995). The following conclusion can be drawn from the plots:

1. The Viterbi soft-decision decoding plus correlated diversity system is more effective relative to a coding alone system, even with dual diversity with correlation coefficient as high as $\rho_s = 0.9$. It can be seen that the performance with correlation coefficient as $\rho_s = 0.5$ does not lose much diversity gain corresponding to the performance with independent diversity ($\rho_s = 0$).
2. Combining a convolutional coding with a diversity system is more effective than using diversity alone within a practical SNR range with $L=2, 4$, and 6 .
3. Combining coding and diversity technique is significant in the conditions where diversity branches are correlated. The gain of combining coding with diversity relative to a diversity alone system seems bigger with branch correlation as $\rho_s = 0.5$ than $\rho_s = 0$.
4. It is found that convolutional coding plus diversity is more effective than block coding plus diversity, which is also discussed in (Chang & McLane, 1995).

In summary, the performance of soft-decision Viterbi decoding, non-coherent demodulator can be upper-bounded when the diversity branches are correlated. Such correlation does not strongly degrade the performance of the coding plus diversity system. The correlation coefficients must be above 0.5 to get appreciable losses. In other words, the convolutional coding and diversity perform effectively when they are used together. This detection method can be used in Multiple-Input and Multiple Output (MIMO) system where multiple antennas are used for diversity at receivers.

4. Antenna switch diversity for practical situations

For antenna diversity, the multiple RF (Radio Frequency) front-end paths associated with multiple antennas are costly in terms of size, power and complexity. Antenna selection is a scheme to reduce the unnecessary RF front-end paths and to capture many of the advantages of diversity systems. This section of the chapter presents an antenna switch algorithm as one kind of selection diversity methods. This algorithm minimizes the unnecessary frequent switches because the switches between diversity branches could bring extra noise and errors to the detector. This algorithm is robust in non-ideal antenna situations where correlation and average power imbalance among antennas are unavoidable. The performance of this antenna switch algorithm is shown with sizable gain in those situations.

4.1 The switch diversity strategy

Optimum selection diversity is defined to choose the antenna/RF path with the highest SNR, and to perform detection based on the signal from the selected path (Simon & Alouini, 2002). Theoretically this leads the optimal results. However, a suboptimal version of selection diversity, known as scan diversity, tests the paths one by one until one is found with SNR above a predetermined threshold. This path is used for detection (Sanayei & Nosratinia, 2004).

However, some practical issues are overlooked in those antenna selection algorithms. The RF switches available with current technologies are far from ideal, which may offset some of the advantage of antenna selection if the antenna switching is frequently performed. Another important shortcoming of the practical switches is their transfer attenuation, which must be compensated by more power from the output stage amplifier of the transmitter and/or by a more sensitive low noise amplifier at the receiver (Sanayei & Nosratinia, 2004). The antenna switch algorithm presented in this section will reduce the unnecessary switches and maximize the overall diversity gain under non-ideal conditions.

This antenna switch algorithm is developed and inspired by a philosophy of selection and switching positions. For example, “Should you always monitor the job market and switch to the best job available to you?”, “Is the grass always greener on the other side of the fence?”, “Is the *best* performing position you found at the switching moment going to last long?” Since switching incurs some transition difficulties and losses as well as the cost and price for monitoring multiple positions/branches, constantly switching to the currently measured *best* position/branch may not be the best strategy. When should the switch be performed then? The answer is when the current position/branch is *bad* enough. Now, only one position/branch, which is the currently working position/branch, needs to be monitored. Switching to an available position/branch occurs only when the current position/branch is found to be unacceptable. The above strategy has been put into the antenna diversity algorithm in wireless communication and was simulated to be a better practical switch method not only in our life situations, but also in diversity systems.

4.2 The switch diversity algorithm

Fig. 8 shows this antenna switch scheme. Multiple receiver antennas are used to receive the signals from possible multiple transmitter antennas. Here only one of the RF paths is selected to be used in signal detection for the simplicity of illustration. And only the selected RF path is monitored and measured in terms of signal strength.

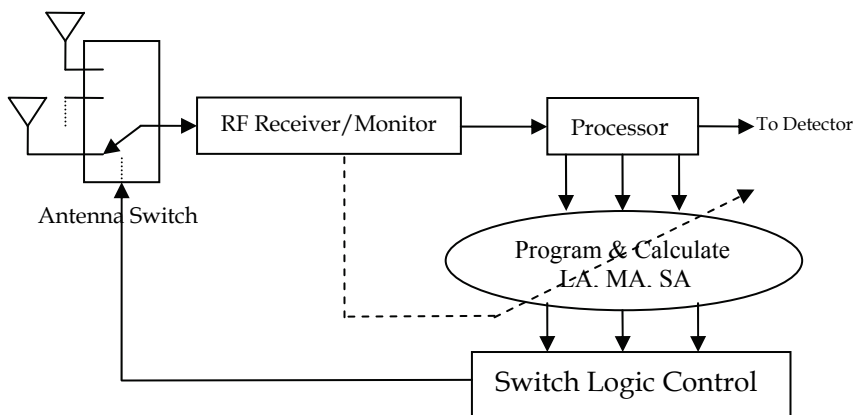


Fig. 5. Antenna Switch Diversity for Wireless Channel

The switch threshold is determined in real-time by moving averages of the measured signal power in long-term, medium-term and short term. In mobile wireless communications, there are fading, Doppler effect, and multipath effect, etc. The long-term average of signal power (LA) characterizes the average signal quality in recent environment. The short-term average of signal power (SA) gives the instantaneous signal strength and the depth of fading at the instance. The medium-term average of signal power (MA) tries to quickly assess the overall signal strength. Comparing MA and LA, the knowledge of the speed of the wireless fading channel can be gained. The periods of long-term, short-term and medium-term can be programmed depending on the speed of mobile and channel condition, the modulation schemes, and the transmission bit/symbol rate.

The switch decision can be designed based on the algorithm that is patented in a US patent (Chang, 1997). The switch decision or threshold can be also made at the signal processor and switch logic control unit of the receiver, which is programmable through the RF path monitor as in Fig. 5. The decoding information and BER measure, which indicate the wireless channel conditions, can be utilized in program the terms used in calculating the LA, MA and SA.

4.3 Practical situations discussion

The switch algorithm presented here is preferable to the theoretically optimal selection diversity due to several reasons. 1) The optimal selection algorithm needs monitoring all the diversity branches at all time, which results in needing multiple RF-front receiver/monitor paths. And it leads to increase the cost and size of the receiver. 2) The optimal selection introduces a lot of switch transitions. The transitions can cause amplitude discontinuous and phase distortion, which then will bring noise and errors to the signal detection. Switch only at deep fades as in the presented switch algorithm reduces the unnecessary switches but keeps the most of the diversity gain.

This switch algorithm is suitable for the practical situation where diversity correlation and power imbalance are unavoidable. This kind of non-ideal antenna condition impact on diversity gains of selection diversity has been discussed in many published papers (Simon & Alouini, 2002, Dietze et al., 2002, Chang & McLane, 1997, Zhang, 2002, Mallik et al., 2000). The switch algorithm presented here is designed in removing the deep fades which are the causes of the major detection errors. As discussed in Section 2 these deep fades are comparatively rare events in probabilistic terms. Therefore, even when two receiver diversity branches have a fairly high overall correlation and large average power imbalance, there is a low probability that both branches will be suffering this rare event (i.e. deep fading) simultaneously. An example is shown in Fig. 3. That is why the switch algorithm which only switches at deep fades is insensitive to diversity correlation and power imbalance. This intuitive prediction becomes convincing by the simulation results presented in (Vasana, 2005).

This switch algorithm is also workable for the practical situation where channel conditions are unknown. The monitoring and comparing of LA, MA and SA can be made to estimate the channel conditions of fast fading and Doppler effects, etc. Therefore, this switch diversity can be self adjusting and adopting to the transmission environment change.

In summary, this antenna switch diversity presented here is cost-effective and robust. The antenna selection at the front of the receiver reduces the unnecessary RF front-end paths but

captures the diversity effect of the multiple antennas. This scheme is designed to switch only when it is necessary and therefore minimizes the switch noise and transition errors. The switch control decisions are made based on a few measured parameters to capture the real-time dynamic channel conditions. Those parameters are easy to be cooperated with BER and soft-decision decoding information to make more sophisticated switch control decisions. The algorithm is robust in practical situations, such as non-ideal diversity situations, no channel knowledge, and fast fading, etc. This is demonstrated in system simulations in (Vasana, 2005).

5. Conclusion

This chapter has discussed the diversity and coding methods to combat fading in wireless communication. The fading models which are used in the analysis are Rayleigh fading with non-LOS and Rician fading with LOS. The diversity branches are considered with non-ideal conditions such as correlation and power imbalance. In spite of all these non-ideal diversity conditions, there is still significant diversity gain when applying antenna diversity reception to practical mobile or wireless radio systems.

An intuitive explanation for many of the diversity non-ideal conditions so they can have acceptable reception is given here. The diversity gain is only achieved when there is deep fading, which does not occur at all-time moments. The overall time correlation and power imbalance will affect, but will not totally eliminate, the diversity gain at those deep fading moments. Section 2 discussed the effect of diversity with various non-ideal conditions - correlated or unbalanced diversity branches for Rayleigh fading signals both in theory and in simulation results.

A linear diagonalization transformation is illustrated in Section 2 & 3. This transformer not only can transfer the correlated and balanced diversity branches to the uncorrelated and unbalanced branches, but also can transfer the unbalanced and uncorrelated diversity branches to the balanced and correlated branches. This transformation technology is especially effective when the noise components have the similar correlation as the signal components.

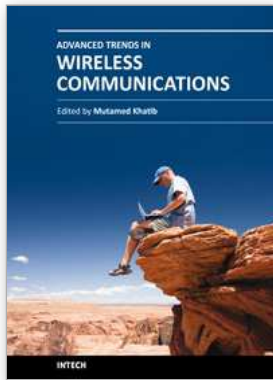
In Section 3 the performance upper-bound of soft-decision Viterbi decoding, non-coherent demodulator is derived when the diversity branches are correlated. Numerical calculation shows that such correlation does not strongly degrade the performance of the soft-decision decoding system. The correlation coefficients must be above 0.5 to get noticeable losses in the coding & diversity gain. In other words, the combination of the convolutional coding and diversity performs effectively to combat fading in wireless communication with practical non-ideal diversity conditions.

The antenna switch diversity, presented in Section 4, is a practical and cost-effective modification to the optimal selection diversity. The antenna selection at the front-end of the receiver reduces the unnecessary RF paths but captures the diversity gain of multiple antennas. This algorithm is designed to switch only when the current path is in *bad* conditions (e.g. deep fading), and therefore minimizes the extensive switch noise and transition errors. One algorithm shows how the switch control decisions are made based on the real-time dynamic channel conditions. The algorithm is robust in practical conditions, such as non-ideal antenna diversity, no channel knowledge and fast fading, etc. The performance improvements are demonstrated in the system simulations.

6. References

- Bi, G.; Yang, C. & Fang, L. (2003). Reply to "Comments on 'New method of performance analysis for diversity reception with correlated Rayleigh-fading signals'", *IEEE transactions on vehicular technology*, vol.52, no.3, May 2003.
- Chang, S. et al. (1997). Communication Device Having Antenna Switch Diversity and Method Therefore, *US Patent PN# 5,692,019*, Issued in 1997.
- Chang, C-Y. S. & McLane, P. J. (1997). Bit-Error-Probability for Noncoherent Orthogonal Signals in Fading with Optimum Combining for Correlated Branch Diversity, *IEEE transactions on information theory*, vol.43, no.1, January 1997.
- Chang, C. S. & McLane, P. J. (1995). Convolutional Codes with Correlated Diversity and Non-Coherent Orthogonal Modulation, *IEEE International Conference on Communications*, Seattle, June 1995.
- Chang, C. S. & McLane, P. J. (1994). Bit-error-probability for non-coherent orthogonal signals in fading with optimum combining for correlated branch diversity, *IEEE Trans. on Information Theory*, Vol. 43, No.1, January 1994.
- Dietze, K.; Dietrich, C. B. & Stutzman, W. L. (2002). Analysis of a two-branch maximal ratio and selection diversity system with unequal (SNR)s and correlated inputs for a Rayleigh fading channel, *IEEE transactions on wireless communications*, vol.1, no.2, April 2002.
- Fang, L.; Bi, G. & Kot, A. C. (2000). New method of performance analysis for diversity reception with correlated Rayleigh-fading signals, *IEEE transactions on vehicular technology*, vol.49, no.5, September 2000.
- Gradshteyn, I. S. & Ryzhik, I. M. (1980). *Table of Integral Series and Products*, New York, Academic Press Inc., 1980.
- Loyka, S. & Tellambura, C. & Kouki, A. etc. (2003). Comments on 'New method of performance analysis for diversity reception with correlated Rayleigh-fading signals', *IEEE transactions on vehicular technology*, vol.52, no.3, May 2003.
- Mallik, R. K., Win, M. Z., & Winters, J. H. (2002). Performance of dual-diversity predetection EGC in correlated Rayleigh fading with unequal branch SNR, *IEEE transactions on communications*, vol.50, no.7, July 2002
- Mallik, R. K.; Win, M. Z. & Winters, J. H. (2000). Performance of predetection dual diversity in correlated Rayleigh fading: EGC and SD, *GLOBECOM '00, IEEE Global Telecommunications Conference*, San Francisco, 27 November-1 December, 2000.
- Modestino, J. W. & Mui, S. Y. (1979). Convolutional code performance in the Rician fading channel, *IEEE Trans. on Commun.*, Vol. 24, June 1976
- Proakis, J. (1989). *Communications*, 2nd Edition, McGraw-Hill, New York, 1989.
- Sanayei, S. & Nosratinia, A. (2004). Antenna Selection in MIMO Systems, *IEEE Communications Magazine*, vol.42, no.10, October 2004.
- Simon, M. K. & Alouini, M. (2002). A Compact Performance Analysis of Generalized Selection Combining with Independent but Non-identically Distributed Rayleigh Fading Paths, *IEEE Trans. Commun.*, vol.50, no.9, Sept. 2002.
- Vasana, S. (2008). Modeling and Simulation of the Conversion of Correlated and Unbalanced Antenna Diversity Systems, *International Journal of Modeling and Simulation*, Vol.28, No.1, 2008.

- Vasana, S. (2005). Antenna Switch Algorithm in MIMO Systems, *Proceedings of IASTED International Conference on Communication Systems and Applications (CSA)*, July 2005.
- Viterbi, A. & Omura, J. (1979). *Principles of Communications*, McGraw-Hill, New York, 1979.
- Zhang, Q. T. (2002). Generic SER formulas for noncoherent MFSK with L diversity on various correlated fading channels, *ICC 2002, IEEE International Conference on Communications*, April-2 May, 2002, New York, NY, USA.



Advanced Trends in Wireless Communications

Edited by Dr. Mutamed Khatib

ISBN 978-953-307-183-1

Hard cover, 520 pages

Publisher InTech

Published online 17, February, 2011

Published in print edition February, 2011

Physical limitations on wireless communication channels impose huge challenges to reliable communication. Bandwidth limitations, propagation loss, noise and interference make the wireless channel a narrow pipe that does not readily accommodate rapid flow of data. Thus, researches aim to design systems that are suitable to operate in such channels, in order to have high performance quality of service. Also, the mobility of the communication systems requires further investigations to reduce the complexity and the power consumption of the receiver. This book aims to provide highlights of the current research in the field of wireless communications. The subjects discussed are very valuable to communication researchers rather than researchers in the wireless related areas. The book chapters cover a wide range of wireless communication topics.

How to reference

In order to correctly reference this scholarly work, feel free to copy and paste the following:

(Chun-Ye) Susan Vasana (2011). Diversity and Decoding in Non-Ideal Conditions, Advanced Trends in Wireless Communications, Dr. Mutamed Khatib (Ed.), ISBN: 978-953-307-183-1, InTech, Available from: <http://www.intechopen.com/books/advanced-trends-in-wireless-communications/diversity-and-decoding-in-non-ideal-conditions>

INTECH

open science | open minds

InTech Europe

University Campus STeP Ri
Slavka Krautzeka 83/A
51000 Rijeka, Croatia
Phone: +385 (51) 770 447
Fax: +385 (51) 686 166
www.intechopen.com

InTech China

Unit 405, Office Block, Hotel Equatorial Shanghai
No.65, Yan An Road (West), Shanghai, 200040, China
中国上海市延安西路65号上海国际贵都大饭店办公楼405单元
Phone: +86-21-62489820
Fax: +86-21-62489821

© 2011 The Author(s). Licensee IntechOpen. This chapter is distributed under the terms of the [Creative Commons Attribution-NonCommercial-ShareAlike-3.0 License](#), which permits use, distribution and reproduction for non-commercial purposes, provided the original is properly cited and derivative works building on this content are distributed under the same license.